Chinese Medical Journal®

B7-H3 confers stemness characteristics to gastric cancer cells by promoting glutathione metabolism through AKT/pAKT/Nrf2 pathway

Lu Xia[1,2,3,4], Yuqi Chen[1,2], Juntao Li[1,2], Jiayu Wang[1,2], Kanger Shen[1,2], Anjing Zhao[1,2,5], Haiyan Jin[1,3,4], Guangbo Zhang[1,3,4], Qinhua Xi[2], Suhua Xia[3,6], Tongguo Shi[1,3,4], Rui Li[2,3,4]

[1]Jiangsu Institute of Clinical Immunology, The First Affiliated Hospital of Soochow University, Suzhou, Jiangsu 215000, China;
[2]Department of Gastroenterology, The First Affiliated Hospital of Soochow University, Suzhou, Jiangsu 215000, China;
[3]Jiangsu Key Laboratory of Clinical Immunology, Soochow University, Suzhou, Jiangsu 215000, China;
[4]Jiangsu Key Laboratory of Gastrointestinal Tumor Immunology, The First Affiliated Hospital of Soochow University, Suzhou, Jiangsu 215000, China;
[5]Department of Oncology, The First Affiliated Hospital of Naval Military Medical University, Shanghai 200433, China;
[6]Department of Oncology, The First Affiliated Hospital of Soochow University, Suzhou, Jiangsu 215000, China.

Abstract

Background: Cancer stem-like cells (CSCs) are a small subset of cells in tumors that exhibit self-renewal and differentiation properties. CSCs play a vital role in tumor formation, progression, relapse, and therapeutic resistance. B7-H3, an immunoregulatory protein, has many protumor functions. However, little is known about the mechanism underlying the role of B7-H3 in regulating gastric cancer (GC) stemness. Our study aimed to explore the impacts of B7-H3 on GC stemness and its underlying mechanism.

Methods: GC stemness influenced by B7-H3 was detected both *in vitro* and *in vivo*. The expression of stemness-related markers was examined by reverse transcription quantitative polymerase chain reaction, Western blotting, and flow cytometry. Sphere formation assay was used to detect the sphere-forming ability. The underlying regulatory mechanism of B7-H3 on the stemness of GC was investigated by mass spectrometry and subsequent validation experiments. The signaling pathway (Protein kinase B [Akt]/Nuclear factor erythroid 2-related factor 2 [Nrf2] pathway) of B7-H3 on the regulation of glutathione (GSH) metabolism was examined by Western blotting assay. Multi-color immunohistochemistry (mIHC) was used to detect the expression of B7-H3, cluster of differentiation 44 (CD44), and Nrf2 on human GC tissues. Student's *t*-test was used to compare the difference between two groups. Pearson correlation analysis was used to analyze the relationship between two molecules. The Kaplan–Meier method was used for survival analysis.

Results: B7-H3 knockdown suppressed the stemness of GC cells both *in vitro* and *in vivo*. Mass spectrometric analysis showed the downregulation of GSH metabolism in short hairpin B7-H3 GC cells, which was further confirmed by the experimental results. Meanwhile, stemness characteristics in B7-H3 overexpressing cells were suppressed after the inhibition of GSH metabolism. Furthermore, Western blotting suggested that B7-H3-induced activation of GSH metabolism occurred through the AKT/Nrf2 pathway, and inhibition of AKT signaling pathway could suppress not only GSH metabolism but also GC stemness. mIHC showed that B7-H3 was highly expressed in GC tissues and was positively correlated with the expression of CD44 and Nrf2. Importantly, GC patients with high expression of B7-H3, CD44, and Nrf2 had worse prognosis ($P = 0.02$).

Conclusions: B7-H3 has a regulatory effect on GC stemness and the regulatory effect is achieved through the AKT/Nrf2/GSH pathway. Inhibiting B7-H3 expression may be a new therapeutic strategy against GC.

Keywords: B7-H3; Cancer stem-like cells; Glutathione; Protein kinase B; Nuclear factor erythroid 2-related factor 2; Gastric cancer

Introduction

Gastric cancer (GC) is prevalent in many parts of the world.[1] It is the third leading cause of cancer-related death worldwide, and patients diagnosed with GC generally have poor prognosis because they are usually found at an advanced stage.[2,3] Cancer stem-like cells (CSCs) are a subpopulation of cells that reside in tumors; these

Access this article online

Quick Response Code:

Website: www.cmj.org

DOI: 10.1097/CM9.0000000000002772

Correspondence to: Rui Li, Department of Gastroenterology, The First Affiliated Hospital of Soochow University, 188, Shizi Road, Suzhou, Jiangsu 215000, China
E-Mail: lrhcsz@163.com;
Tongguo Shi, Jiangsu Institute of Clinical Immunology, The First Affiliated Hospital of Soochow University, 178, East Ganjiang Road, Suzhou, Jiangsu 215000, China
E-Mail: shitg@suda.edu.cn;
Suhua Xia, Department of Oncology, The First Affiliated Hospital of Soochow University, 188 Shizi Road, Suzhou, 215000, China
E-Mail: xiasuhua@suda.edu.cn

Chinese Medical Journal 2023;136(16)
Received: 27-10-2022; **Online:** 24-07-2023 **Edited by:** Jinjiao Li and Yuanyuan Ji

cells have self-renewal ability and high tumorigenic potency.[4,5] A large body of evidence has confirmed that CSCs contribute to the initiation, relapse, metastasis, and therapeutic resistance of multiple malignancies including GC.[6-9] Therefore, a detailed understanding of the molecular mechanisms that modulate the stem-like properties of GC cells is urgently needed.

B7-H3, also known as CD276, is an immunoregulatory protein belonging to the B7 family.[10] Apart from its role in regulating immunological function in the tumor microenvironment,[11,12] B7-H3 also has non-immunological pro-tumorigenic functions, including promoting endothelial-to-mesenchymal transition (EMT),[13] chemoresistance,[14] and angiogenesis[15] and affecting cancer cells' metabolism.[16] Recently, the biological function of B7-H3 in controlling the stemness of cancer cells has received increasing attention.[17-21] However, the role and underlying molecular mechanism by which B7-H3 modulates the stemness of GC cells remain unknown.

This study aimed to investigate the effect of B7-H3 on the stemness characteristics of GC cells and the mechanism of its regulation of GC cell stemness. Hopefully, the results of this study may provide a potential new target for the treatment of GC patients.

Methods

Cell culture, transfection, and infection

HGC-27 and MKN-28 cell lines (Chinese Academy of Science Cell Bank, Shanghai, China) were separately cultured in Dulbecco's Modified Eagle Medium (DMEM, EallBio, Beijing, China) and Roswell Park Memorial Institute (RPMI) 1640 (EallBio) containing 10% fetal bovine serum (FBS, EallBio) and 1% penicillin-streptomycin (Beyotime, Shanghai, China) at 37°C in a humidified atmosphere with 5% CO_2.

Small interfering RNA (siRNA) for B7-H3 (B7-H3 siRNA-1 [5′-GCUGUCUGUCUGUCUCAUUTT-3′], siRNA-2 [5′-GUGCUGGAGAAAGAUCAAATT-3′]), and control siRNA were purchased from GenePharma Co. Ltd. (Suzhou, China). Lipofectamine 2000 (Invitrogen, Carlsbad, CA, USA,) was used to transfect HGC-27 and MKN-28 cell lines with B7-H3 siRNA according to the manufacturer's protocol. The transfection efficiency was confirmed by Western blotting.

Lentiviruses carrying B7-H3 short hairpin RNA (shRNA) or B7-H3 overexpression vector were purchased from GenePharma Co., Ltd. (Suzhou, China). An empty backbone vector was used as a control. In brief, HGC-27 and MKN-28 cells were grown to 30% confluence in 12-well plates and were infected with lentiviral particles (MOI [Multiplicity of Infection]: 20). The infection efficiency was determined by counting green fluorescent protein-expressing cells under a fluorescence microscope after 72 h infection, and the subsequent Western blotting.

RNA isolation and real-time quantitative polymerase chain reaction (RT-qPCR)

Total RNA was extracted from cells using TRIzol reagent (Vazyme, Nanjing, China) according to the manufacturer's instructions. To analyze individual gene expression levels, 1 μg of total RNA was reverse-transcribed into complementary DNA (cDNA) using Monscrip™ RTase III (Monad, Suzhou, China) in a volume of 20 μL. RT-qPCR was performed on a CFX96 Touch™ real-time PCR system (Bio-Rad, CA, USA) using AceQ universal SYBR qPCR (Monad) according to the manufacturer's protocol. β-actin was chosen to be a constitutive control. Samples and reference genes were analyzed in triplicate. The primer sequences used for RT-qPCR are provided in Supplementary Table 1, http://links.lww.com/CM9/B628.

Western blotting

HGC-27 and MKN-28 cells were lysed with cell lysis buffer (Beyotime) containing protease inhibitors and phosphatase inhibitors (Beyotime) at 4°C. Protein concentrations were examined with Enhanced bicinchoninic acid Protein Assay Kit (Beyotime). Equal amounts of protein were separated by 10% sodium dodecyl sulfate-polyacrylamide gel electrophoresis (New Cell & Molecular Biotech, Suzhou, China) and transferred to 0.45 μm polyvinylidene difluoride membranes (GE Healthcare Life Science, Freiburg, Germany). Then the membranes were blocked with 5% bovine serum albumin blocking buffer (Fcmacs, Nanjing, China) for 1.5 h and incubated with primary antibodies at 4°C overnight. The antibodies for Western blotting were as follows: B7-H3 (Proteintech, Wuhan, China), CD133 (Proteintech), CD44 (Proteintech), Sox2 (SRY-box transcription factor 2, Proteintech), Nrf2 (Proteintech), AKT (Beyotime), pAKT (Phospho-protein kinase B, Cell Signaling Technology, Danvers, MA, USA), β-actin (ImmunoWay, Plano, TX, USA), and GAPDH (Glyceraldehyde-3-phosphate dehydrogenase, Proteintech). The next day, the membranes were washed and then incubated with the corresponding Horseradish Peroxidase-conjugated secondary antibodies at room temperature for 1 h. Finally, the membranes were visualized with Electochemiluminescence (ECL) reagents (New Cell & Molecular Biotech) using a Chemi Doc™ MP Imaging System (Bio-Rad, Hercules, CA, USA).

Sphere formation assay

A spheroid-formation assay was used to detect the stemness of GC cells. Specifically, HGC-27 and MKN-28 cells were cultured in ultra-low-attachment 96-well plates (Corning, Corning, NY, USA) with serum-free Dulbecco's Modified Eagle Medium (DMEM) or RPMI-1640, containing EGF (epidermal growth factor, 20 ng/mL, Beyotime), bFGF (basic fibroblast growth factor, 20 ng/mL, Beyotime), B27 (2%, Gibco, Grand Island, NY, USA), insulin (4 μg/mL, Beyotime), and penicillin-streptomycin (1%). For HGC-27 cells, the concentrations of cells

were chosen as 100 cells/well, 80 cells/well, and 60 cells/well, while the concentrations of MKN-28 cells were chosen as 160 cells/well, 140 cells/well, and 120 cells/well. Each cell concentration had 10 replicates. After 10–14 days, light microscopy was used to count the sphere numbers and to observe the sphere size.

Liquid chromatography–mass spectrometry/mass spectrometric (LC–MS/MS) analysis

To identify the metabolites modulated by B7-H3, untargeted metabolomics analysis using shB7-H3 HGC-27 cells and negative control HGC-27 cells was performed by BGI (Shenzhen, China). In brief, high-resolution mass spectrometer Q Exactive HF (ThermoFisher Scientific, Waltham, MA, USA) was used to collect data from positive and negative ions. Compound Discover 3.1 (Thermo Fisher Scientific) was used for LC–MS/MS data processing. A self-developed R package[22] and the metabolome bioinformatic analysis pipeline were used for data preprocessing, statistical analysis, metabolite classification annotations, and functional annotations. Principal component analysis (PCA) was used for multivariate raw data to analyze the groupings, trends, and outliers of the observed variables in the data set. Partial lest squares method-discriminant analysis (PLS-DA) (VIP $\geq$1 of the first two principal components of the model), fold change (FC, $\geq$2 or $\leq$0.5), and Student's *t*-test (q <0.05) were used to screen for differential metabolites.

GSH content and Glutathione-S-transferase (GST) activity detection

The content of GSH and the enzyme activity of GST in cells were detected by colorimetric method with test kits produced by Nanjing Jiancheng Bioengineering Institute (Nanjing, China). GSH content and GST activity were measured by protein concentration.

Xenograft tumor

All animal experiments were performed under the protocol approved by the Institutional Animal Care and Use Committee at Soochow University (Suzhou, China) (Ethical approval number, 202206A0710). Six- to eight-week-old female BALB/c athymic nude mice were purchased from the Experimental Animal Center of Chinese Academy of Medicine Sciences of Soochow University and maintained in a specific pathogen-free (SPF) environment. All animals were randomly assigned to each group. To explore whether B7-H3 could affect GC stemness *in vivo*, different concentrations (1×10^6/mL, 1×10^5/mL) of control HGC-27 cells and shB7-H3 HGC-27 cells were subcutaneously injected into the right and left flanks of each mouse. To investigate whether GSH metabolism was involved in B7-H3-mediated GC stemness *in vivo*, mice were randomly divided into two groups, the B7-H3-overexpressing HGC-27 (B7-H3) and B7-H3 + buthionine sulfoximine (BSO) groups. BSO is an inhibitor of GSH synthesis. Mice in the B7-H3 + BSO group were intraperitoneally injected with BSO at a dose of 500 mg/kg every four days. The mice in B7-H3 group received vehicle control. Tumor volumes were calculated by the formula V (mm^3) = L (mm) × S^2 (mm^2)/2, where L and S represent the longest and shortest perpendicular tumor diameters, respectively.

Flow cytometry

To detect the expression of CD133 in GC cells, a PE-conjugated antibody against CD133 (BioLegend, USA) was used to stain the cells. In brief, after digestion with trypsin and centrifugation, cells were resuspended in phosphate buffered saline (PBS) and stained with CD133 antibody for 25 min at 4°C, followed by analysis using flow cytometry.

Detection of intracellular reactive oxygen species (ROS)

Dihydroethidium (DHE, Beyotime) was used to measure intracellular ROS level. In brief, cells were incubated with DHE at a concentration of 5 μmol/L for 30 min at 37°C. All subsequent steps were performed in the dark. After 30 min of incubation, the cells were washed in PBS, and then single-cell suspensions were analyzed using flow cytometry. Data analysis was performed using FlowJo software (Version 7.6, TreeStar, Ashland, OR, USA).

Chemo-sensitivity assay

Cell viability was examined by Cell Counting Kit-8 (CCK-8, New Cell & Molecular Biotech) assay. In brief, GC cells were seeded in 96-well plates (3000 cells/well). After the cells were treated with different concentrations of 5-Fluorouracil (5-FU) for 24 h, the number of viable cells was assessed using the Cell Counting Kit-8. The absorbance of each well was measured at a wavelength of 450 nm.

Hematoxylin–eosin (HE) and immunohistochemistry (IHC) staining

Histological changes in xenograft tumor tissues were assessed by hematoxylin and eosin staining using a kit (Beyotime) according to the manufacturer's instructions. IHC was performed as previously described.[23] In brief, after deparaffinization and rehydration, xenograft tumor samples were treated with 10 mmol/L sodium citrate buffer for antigen retrieval. Then, the sections were incubated with B7-H3 antibody (Proteintech, 1:1000) and CD44 antibody (Proteintech, 1:1000) overnight at 4°C. This step was followed by incubating with the HRP-labeled secondary antibody. A semiquantitative immunoreactive score (IRS) system was used to analyze the B7-H3 and CD44 immunostaining.[15]

Multi-color immunohistochemistry (mIHC) and computer-assisted image analysis

All implications and analyses were performed by Shanghai Outdo Biotech Company (Shanghai, China). Ethical approval (No. YB M-05-02) was obtained from the Ethics Committee of Shanghai Outdo Biotech

Company. mIHC was conducted by using an Opal7-color Manual IHC Kit (PerkinElmer, Waltham, MA, USA) combined with automated quantitative analysis (PerkinElmer) according to the manufacturer's protocol to characterize the expression of B7-H3, CD44, and Nrf2 in GC tissue microarrays (TMAs). 4-6-Diamidino-2-phenylindole (DAPI) was used to stain the nucleus, and cytokeratin (CK) was used to distinguish the epithelial cancer cells. Briefly, the GC TMA slide was first dewaxed and dehydrated before incubation in PBS. Next, heat-induced antigen repair was carried out in citric acid buffer followed by incubation with antibodies against B7-H3 (1:100), CD44 (1:20000), Nrf2 (1:1500), and CK (BioDot, Irvine, CA, USA) at room temperature for 1 h. Subsequently, HRP-conjugated secondary-antibodies (PerkinElmer) were used to incubate the GC TMA. The microarray was finally sealed with ProLong Diamond Antifade Reagent with DAPI (Thermo Fisher Scientific).

For imaging analysis, the TissueFAXS system (TissueGnostics Asia Pacific Limited, Beijing, China) was used to carry out the panoramic multispectral scanning of GC TMA slides. Then, the acquired images were analyzed using Strata Quest analysis software (TissueGnostics Asia Pacific Limited).

Statistical analysis

Statistical analysis was performed using Graphpad Prism 8.0 (La Jolla, CA, USA). All the results are presented as mean ± standard deviation (SD). Student's *t*-test was used to compare difference between two groups. Pearson correlation analysis was used analyze the relationship between two molecules. The Kaplan–Meier method was used for survival analysis between B7-H3$^+$CD44$^+$Nrf2$^+$ cells% high (≥lower quartile) and B7-H3$^+$CD44$^+$Nrf2$^+$ cells% low (<lower quartile). Log-rank test was used for comparison of survival curves. All data were obtained in triplicates. P <0.05 was the standard of statistical significance.

Results

B7-H3 influences the stemness of GC cells

As shown in Supplementary Figure 1A, B, http://links.lww.com/CM9/B628, B7-H3 was frequently upregulated in GC cell lines (AGS, MKN-45, HGC-27, MKN-28) compared to the human normal gastric cell line (GES), suggesting that B7-H3 has an important role in GC progression. We then explored whether B7-H3 could affect the stemness of GC cells. As shown in Figure 1A, after knocking down the expression of B7-H3 by using two siRNAs (B7-H3 si-1 and B7-H3 si-2), the expression of CD133, CD44, and Sox2, markers of cancer stem cells, was significantly decreased in HGC-27 and MKN-28 cells. To further confirm our results, we constructed stable B7-H3 knockdown (shB7-H3) HGC-27 and MKN-28 cell lines [Figures 1B,C]. Consistent with Figure 1A, Western blotting revealed that shB7-H3 HGC-27 and MKN-28 cell lines exhibited decreased expression of CD44 and Sox2 [Figure 1C], and the decreased expression of CD133 in shB7-H3 HGC-27 and MKN-28 cell lines was further confirmed by flow cytometry [Figure 1D]. Moreover, sphere formation assays revealed that B7-H3 knockdown significantly suppressed sphere formation in both size and number in these two cell lines [Figure 1E]. Chemo-sensitivity assay showed that shB7-H3 HGC-27 and MKN-28 cells were more sensitive to 5-FU compared with the control cells [Figure 1F]. In addition, the *in vivo* experiment showed that the tumor incidence [Figure 1G] and tumor weight [Figure 1H] were higher in the 1×10^6/mL injection group than in the 1×10^5/mL injection group. Importantly, the expression of CD44 was significantly lower in the shB7-H3 group than in the control group [Figure 1I, Supplementary Figure 1C, http://links.lww.com/CM9/B628]. Collectively, our data suggest that B7-H3 enhanced the stemness of GC cells both *in vitro* and *in vivo*.

B7-H3 regulates GSH metabolism in GC cells

An increasing number of studies have revealed that metabolic reprograming is an important characteristic of cancer cells, and regulates the stem-like properties of cancer cells.[24,25] Thus, we performed untargeted metabolomics analysis using B7-H3 knockdown HGC-27 cells to identify the metabolites [Supplementary Figures 2A,B, http://links.lww.com/CM9/B628] that were modulated by B7-H3. The heatmap and volcano plot showed that among all the metabolites, L-glutathione was reduced, whereas cysteinylglycine and glutamylcysteine, which belong to the GSH metabolic pathway, were significantly reduced, in shB7-H3 HGC-27 cells [Figures 2A,B and Supplementary Figure 3, http://links.lww.com/CM9/B628]. Moreover, consistent with the heatmap and volcano plot results, pathway enrichment analysis demonstrated that the GSH metabolic pathway was dramatically altered in shB7-H3 HGC-27 cell lines [Figure 2C].

To confirm the results of metabolomics, we first measured the mRNA levels of a spectrum of GSH metabolism-related genes in control cells and shB7-H3 cells. As shown in Figure 2D, the mRNA levels of glucose-6-phosphate dehydrogenase, glutathione peroxidase 4, glutathione synthetase, and glutathione S-transferase omega 1 were significantly reduced in shB7-H3 HGC-27 and MKN-28 cells. Additionally, the GSH level and GST enzyme activity were markedly decreased in HGC-27 and MKN-28 cells after B7-H3 knockdown [Figures 2E,F]. However, GPX4 enzyme activity was not affected by B7-H3 knockdown [Supplementary Figure 4, http://links.lww.com/CM9/B628]. Given that GSH plays an important role in buffering intracellular ROS to maintain redox homeostasis in cells,[26,27] we tested the intracellular ROS levels in shB7-H3 HGC-27 and MKN-28 cells using a DHE probe. As shown in Figure 2G, shB7-H3 HGC-27 and MKN-28 cells had higher ROS levels than control cells. Taken together, our data suggest that B7-H3 knockdown markedly suppresses the GSH metabolism in GC cells.

B7-H3 enhances the stemness of GC cells by regulating GSH metabolism

To further verify whether GSH metabolism was related to the B7-H3-mediated stemness of GC cells, we

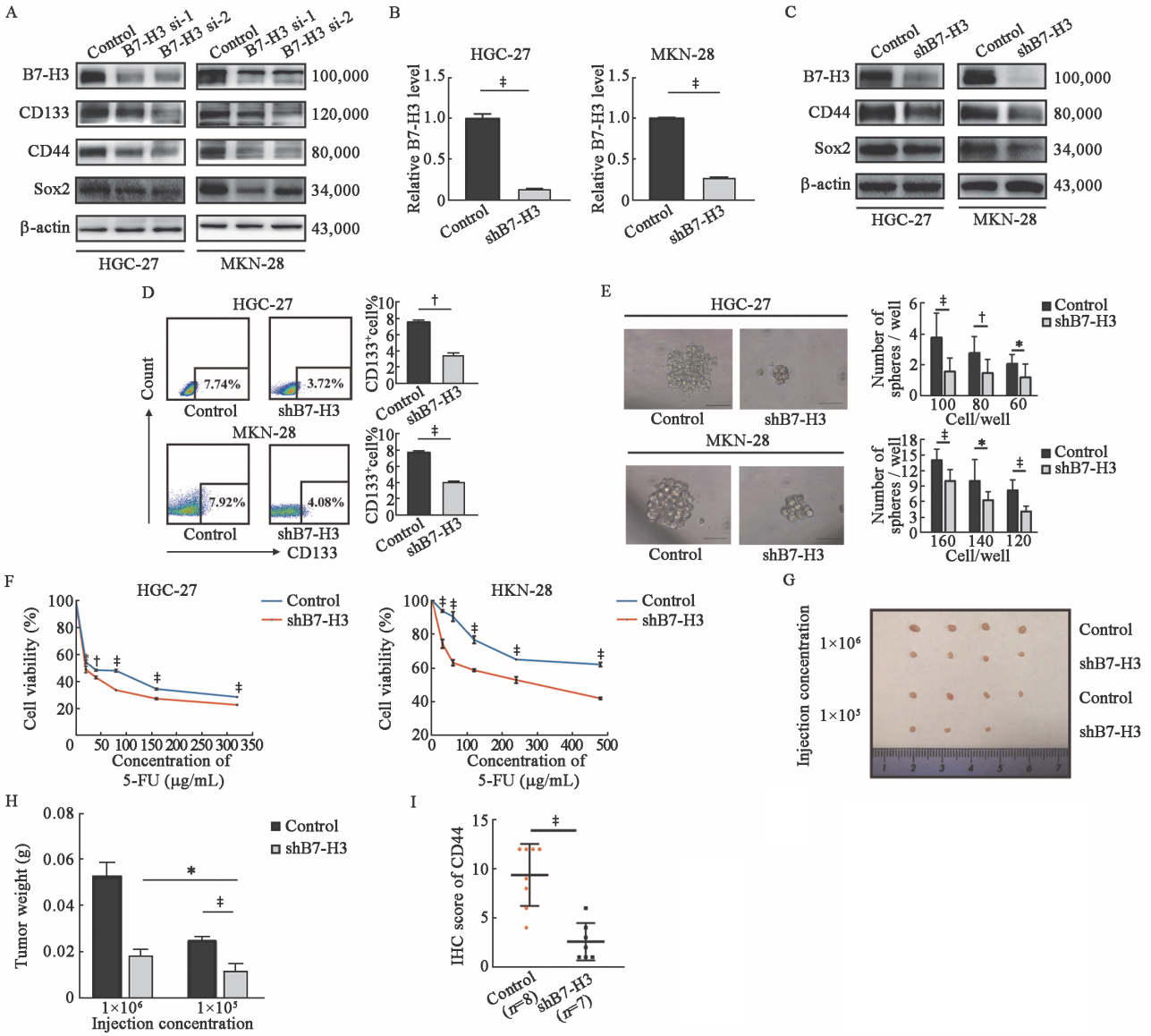

Figure 1: B7-H3 influences the stemness of GC cells. (A) Western blotting of the cancer stemness markers CD133, CD44, and Sox2 in HGC-27 and MKN-28 cell lines after transfection with control siRNA, B7-H3 siRNA-1, or B7-H3 siRNA-2. β-actin served as a loading control. (B) B7-H3 mRNA levels were detected by RT-qPCR in B7-H3 knockdown (shB7-H3) HGC-27 and MKN-28 cell lines and their control cells. (C) Western blotting of the cancer stemness markers CD44 and Sox2 in HGC-27 and MKN-28 cell lines with B7-H3 inhibition and their control cells. β-actin served as a loading control. (D) Flow cytometry analysis of the expression of CD133 in shB7-H3 HGC-27 and MKN-28 cell lines and their control cells. (E) Images and numbers of spheres of shB7-H3 HGC-27 and MKN-28 cell lines and their control cells. Scale bar, 50 μm. (F) Control HGC-27 and MKN-28 cells and shB7-H3 HGC-27 and MKN-28 cells were treated with 5-FU at the indicated concentration for 24 h. Cell viability was tested by CCK8 assay. (G) shB7-H3 HGC-27 cells and their control cells were diluted (1×10^6/mL, 1×10^5/mL) and subcutaneously implanted into the left and right flanks of nude mice. Tumors were observed for 2 months, $n = 4$ for each group. (H) Quantification analysis of tumor weight formed by the control and shB7-H3 HGC-27 cell lines. (I) The expression of CD44 in xenograft specimens of control and shB7-H3 groups based on the IHC results. The data are presented as the means ± SDs. $^*P$ <0.05, $^\dagger P$ <0.01, $^\ddagger P$ <0.001. CCK8: Cell counting Kit-8; CD: Cluster of differentiation; 5-FU: 5-Fluorouracil; GC: Gastric cancer; IHC: Immunohistochemistry; RT-qPCR: Real time quantitative polymerase chain reaction; SDs: Standard deviations; sh: Short hairpin; siRNA: Small interfering RNA; Sox2: SRY-box transcription factor 2.

constructed HGC-27 and MKN-28 cells stably overexpressing B7-H3 [Supplementary Figures 5A, B, http://links.lww.com/CM9/B628]. The results of flow cytometry revealed that treatment with BSO significantly inhibited the increase in CD133 expression caused by B7-H3 overexpression in HGC-27 and MKN-28 cells [Figure 3A]. Moreover, compared with the B7-H3 overexpression group, the sphere-forming ability was markedly downregulated in the B7-H3 + BSO group, as evidenced by the decreased number and size of spheres [Figure 3B]. Chemo-sensitivity assay indicated that the resistance of B7-H3 overexpressing HGC-27 and MKN-28 cells to 5-FU was diminished after the addition of BSO [Figure 3C]. In addition, BSO administration significantly reversed the effect of B7-H3 overexpression on tumorigenesis in nude mice [Figures 3D–F]. The IHC staining showed that the CD44 expression was much higher in the B7-H3 overexpression group than that in the B7-H3 + BSO group [Supplementary Figure 5C, http://links.lww.com/CM9/B628]. The above results suggest that GSH metabolism is critical for the B7-H3-induced stemness of GC cells.

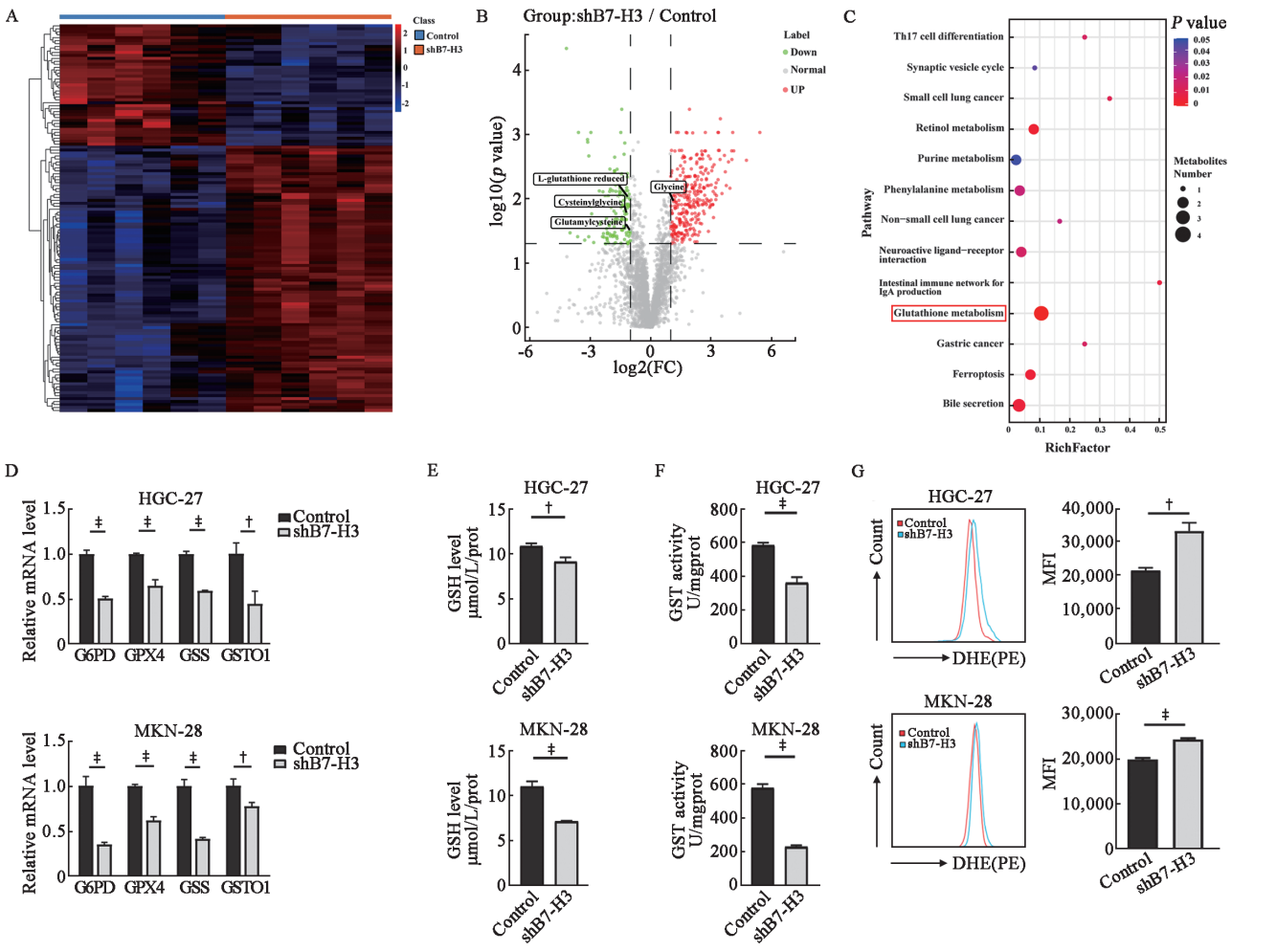

Figure 2: B7-H3 regulates GSH metabolism in GC cells. (A) Heatmap of differentially expressed metabolites between the control and shB7-H3 HGC-27 cell lines. Fold-change ≥2 or ≤0.5, *q*-value <0.05. $N = 6$. (B) Volcano plot of accumulated metabolites that were significantly different between the control and shB7-H3 HGC-27 cell lines. (C) Pathway analysis based on KEGG. The bubble area contributes to the number of metabolites in each pathway, while the color represents significance from highest in red to lowest in blue. (D) Detection of the expression of GSH metabolism-related genes by RT-qPCR in shB7-H3 HGC-27 and MKN-28 cell lines and their control cells. (E,F) GSH content (E) and GST activity (F) in HGC-27 and MKN-28 shB7-H3 cell lines and their control cells. (G) Intracellular ROS level detection in shB7-H3 HGC-27 and MKN-28 cell lines by using a DHE probe. The data are presented as the mean ± SDs. $^{*}P$ <0.05, $^{\dagger}P$ <0.01, $^{\ddagger}P$ <0.001. DHE: Dihydroethidium; FC: Fold change; G6PD: Glucose-6-phosphate dehydrogenase; GC: Gastric cancer; Glutathione S-transferase omega 1; GPX4: Glutathione peroxidase 4; GSH: Glutathione; GSS: Glutathione synthetase; GSTO1; GST: Glutathione S transferase; IgA: Immunoglobulin A; KEGG: Kyoto encyclopedia of genes and genomes; MFI: Mean fluorescence intensity; mRNA: Messenger RNA; PE: Phycoerythrin; prot: protein; ROS: Reactive oxygen species; RT-qPCR: Real time quantitative polymerase chain reaction; SDs: Standard deviations; sh: Short hairpin.

B7-H3 regulates GSH metabolism of GC cells through the AKT/Nrf2 pathway

Previous studies showed that GSH synthesis could be controlled by Nrf2 through the activation of GSH metabolism-related enzymes.[28,29] Besides, Nrf2 has been proven to be related to cancer stemness in multiple ways, such as Nrf2-Keap1-Batch1 signaling pathway and CD133-Nrf2 axis.[30,31] Herein, we speculated that B7-H3 regulated GSH metabolism in GC cells through Nrf2. As shown in Figure 4A, the expression of Nrf2 was downregulated in shB7-H3 HGC-27 and MKN-28 cells. Sulforaphane (SFN), an activator of Nrf2, markedly abolished the inhibitory effects of B7-H3 knockdown on the Nrf2 expression in HGC-27 and MKN-28 cells [Supplementary Figure 6, http://links.lww.com/CM9/B628]. Moreover, SFN increased the GSH level and GST enzyme activity of HGC-27 and MKN-28 cells, which decreased after B7-H3 knockdown [Figures 4B,C].

To further elucidate the mechanism of how B7-H3 regulates Nrf2 expression, we did a literature retrieval. Studies indicated that the AKT/Nrf2 pathway was involved in multiple biological functions in GC.[32,33] Furthermore, B7-H3 overexpression has been shown to significantly activate the AKT pathway in cancers.[34,35] Hence, we hypothesized that B7-H3 could probably control the expression of Nrf2 through the AKT pathway. As the results of Western blot indicated that the expression of pAKT and Nrf2 was elevated in B7-H3 overexpressing cells and could be inhibited by perifosine, an AKT inhibitor [Figure 4D]. Moreover, we observed that treatment with perifosine, an inhibitor of AKT pathway, reversed the effects of B7-H3 overexpression on the GSH metabolism-related genes (*G6PD*, *GPX4*, *GSS*, and *GSTO1*) expression, GSH level, GST enzyme activity, and intracellular ROS levels [Figures 4E–H]. Taken together, the above data illustrate that B7-H3 regulates Nrf2 expression in an AKT-dependent manner,

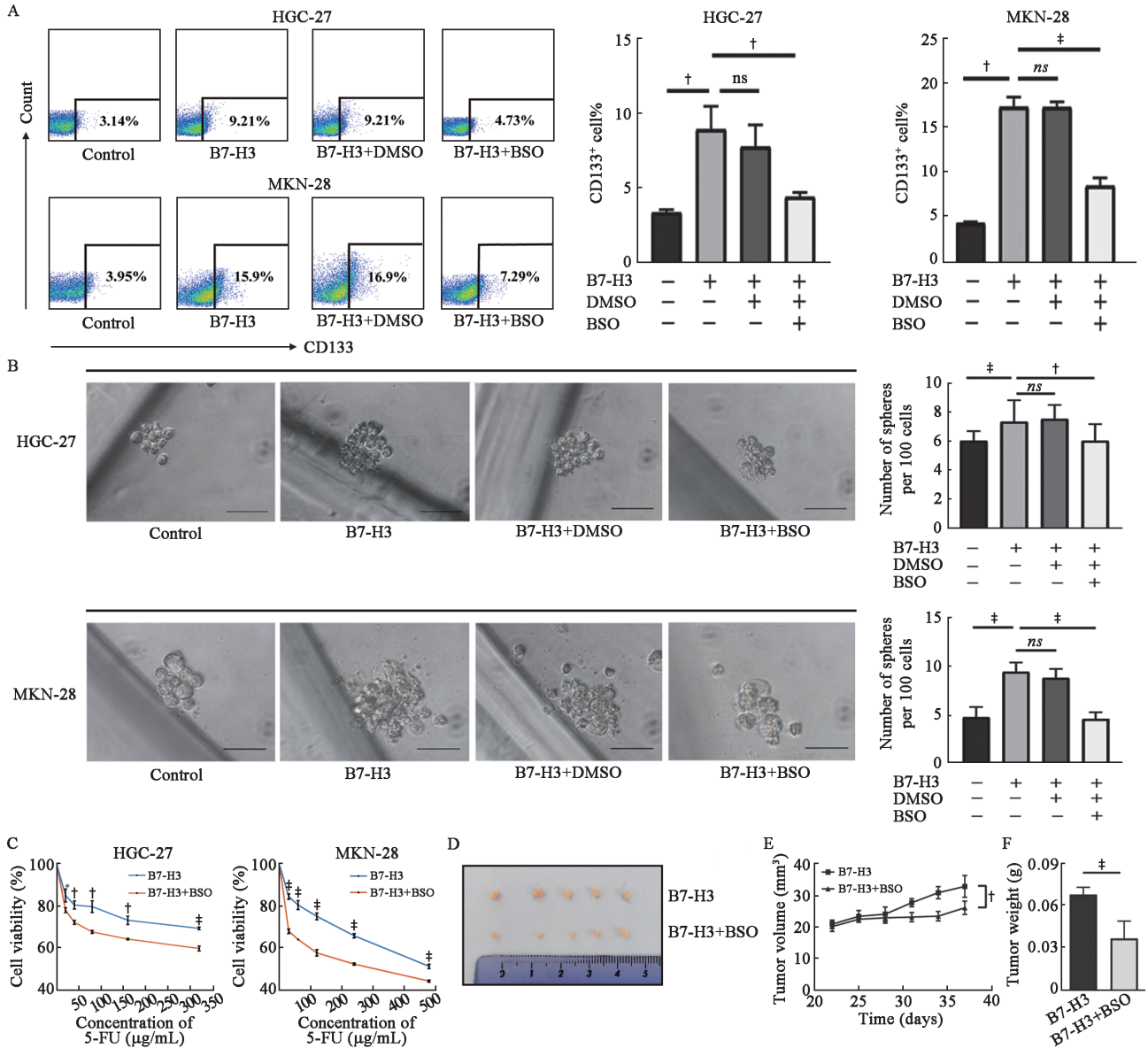

Figure 3: B7-H3 enhances the stemness of GC cells by regulating GSH metabolism. (A) Flow cytometry analysis of CD133 expression on B7-H3-overexpressing HGC-27 and MKN-28 cell lines after treatment with BSO. (B) Images and numbers of spheres of B7-H3-overexpressing HGC-27 and MKN-28 cell lines after treatment with BSO. Scale bar, 50 μm. (C) B7-H3 overexpressing HGC-27 and MKN-28 cells. B7-H3 + BSO HGC-27 and MKN-28 cells were treated with 5-FU at the indicated concentration for 24 h. Cell viability was tested by CCK8 assay. (D) Representative images of B7-H3-overexpressing HGC-27 tumors and B7-H3-overexpressing HGC-27 tumors following BSO treatment (500 mg/kg, $N = 5$). (E, F) Quantification of the size and weight of subcutaneous tumors formed by B7-H3 overexpressing HGC-27 cells and B7-H3 overexpressing HGC-27 cells treated with BSO. The data are presented as the mean ± SDs. $^{*}P$ <0.05, $^{\dagger}P$ <0.01, $^{\ddagger}P$ <0.001. BSO: Buthionine sulfoximine; CD: Cluster of differentiation; DMSO: Dimethyl sulfoxide; GC: Gastric cancer; GSH: Glutatione; *ns*: Not significant; SDs: Standard deviations.

which ultimately contributes to the intracellular GSH metabolism.

The AKT pathway is involved in the B7-H3-induced stemness of GC cells

As shown in Figure 5A, the results of RT-qPCR analysis showed that treatment with perifosine decreased the expression of stemness-related genes including *OCT4, NANOG, ALDH1A3,* and *SOX2*, which were elevated by B7-H3 overexpression. Furthermore, perifosine stimulation abolished the effect of B7-H3 overexpression on the CD133 expression in HGC-27 and MKN-28 cells [Figure 5B]. In addition, the effect of the promotion of B7-H3 overexpression on the sphere formation and drug resistance abilities of HGC-27 and MKN-28 cells was reversed by perifosine [Figures 5C,D].

B7-H3 is highly expressed in GC tissue and is correlated with the expression of CD44 and Nrf2 and the prognosis of GC patients

Next, we investigated the expression of B7-H3 in normal adjacent tissues and tumor tissues. As shown in Figures 6A, B, B7-H3 expression was significantly increased in GC tissues. Moreover, according to the clinical indicators of patients with GC, B7-H3 expression was signifi-

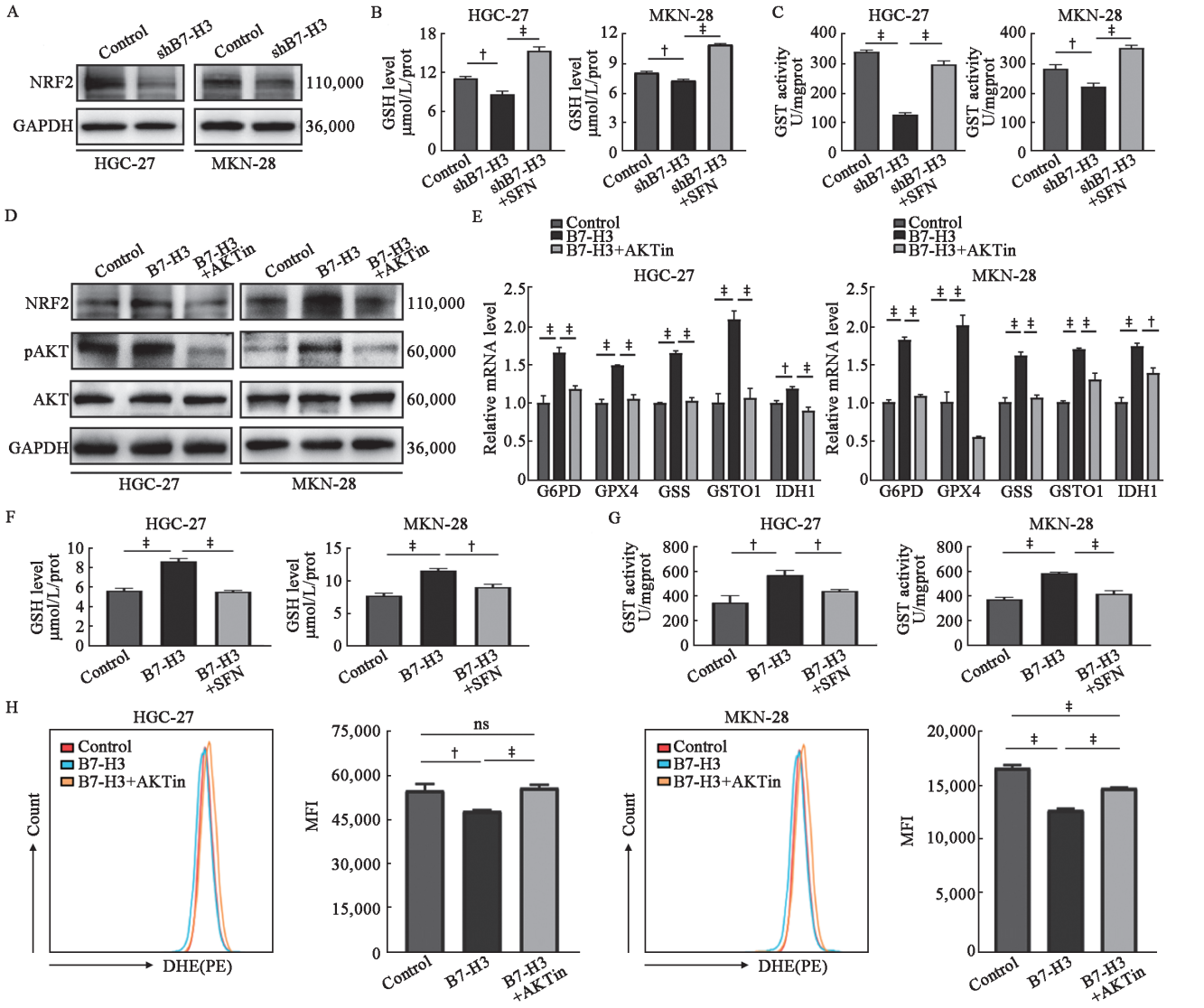

Figure 4: B7-H3 regulates GSH metabolism in GC cells through the AKT/Nrf2 pathway. (A) Western blotting of Nrf2 expression in shB7-H3 HGC-27 and MKN-28 cell lines. (B) GSH levels in shB7-H3 HGC-27 and MKN-28 cell lines after treatment with SFN. (C) GST activity in shB7-H3 HGC-27 and MKN-28 cell lines after treatment with SFN. (D) Western blotting of AKT, pAKT, and Nrf2 expression in the control, shB7-H3, and shB7-H3 + AKTin groups in HGC-27 and MKN-28 cell lines. β-actin served as a loading control. (E) RT-qPCR detection of GSH metabolism-related genes in B7-H3-overexpressing HGC-27 and MKN-28 cell lines after treatment with AKTin. (F) GSH levels in B7-H3-overexpressing HGC-27 and MKN-28 cell lines after treatment with AKTin. (G) GST activity in B7-H3-overexpressing HGC-27 and MKN-28 cell lines after treatment with AKTin. (H) Intracellular ROS level detection in B7-H3-overexpressing HGC-27 and MKN-28 cell lines after treatment with AKTin by using a DHE probe. The data are presented as the mean ± SDs. $^{\dagger}P$ <0.01, $^{\ddagger}P$ <0.001. AKT: Protein kinase B; AKTin: AKT inhibitor; DHE: Dihydroethidium; G6PD: Glucose-6-phosphate dehydrogenase; GAPDH: Glyceraldehyde-3-phosphate dehydrogenase; GC: Gastric cancer; GPX4: Glutathione peroxidase 4; GSH: Glutathione; GSS: Glutathione synthetase; GST: Glutathione S transferase; GSTO1: Glutathione S-transferase omega 1; IDH1: Isocitrate dehydrogenase 1; MFI: Mean fluorescence intensity; ns: Not significant; pAKT: Phospho-protein kinase B; PE: Phycoerythrin; Prot: protein; ROS: Reactive oxygen species; RT-qPCR: Real time quantitative polymerase chain reaction; SDs: Standard deviations; SFN: Sulforaphane; sh: Short hairpin.

cantly correlated with vascular infiltration ($t = 2.61$, $P = 0.01$), perineural invasion ($t = 2.76$, $P < 0.01$), and TNM stage ($t = 3.08$, $P < 0.01$) [Supplementary Table 2, http://links.lww.com/CM9/B628]. We then performed the correlation analysis among B7-H3, CD44, and Nrf2. The results showed that B7-H3 expression was positively associated with the expression of CD44 ($r = 0.53$, $P < 0.01$) and Nrf2 ($r = 0.24$, $P = 0.04$) [Figures 6C,D]. Furthermore, CD44 and Nrf2 also exhibited a positive relationship in GC clinical samples [Figure 6E]. Importantly, patients with high expression levels of B7-H3, CD44, and Nrf2 (B7-H3^{+}CD44^{+}Nrf2^{+} cell% ≥4%) had a worse prognosis than those with low expression levels of B7-H3, CD44, and Nrf2 (B7-H3^{+}CD44^{+}Nrf2^{+} cell% <4%) ($P = 0.05$, Figure 6F). In the meantime, data analysis from the Gene Expression Profiling Interactive Analysis 2 (GEPIA2) database showed that B7-H3 expression had a positive relationship with cancer stem cell markers, including CD44, CD133, epithelial cell adhesion molecule (EpCAM), and Lgr5 [Supplementary Figure 7, http://links.lww.com/CM9/B628]. These findings illustrate the clinical significance of B7-H3, CD44, and Nrf2 in the development of GC and the prognosis of GC patients.

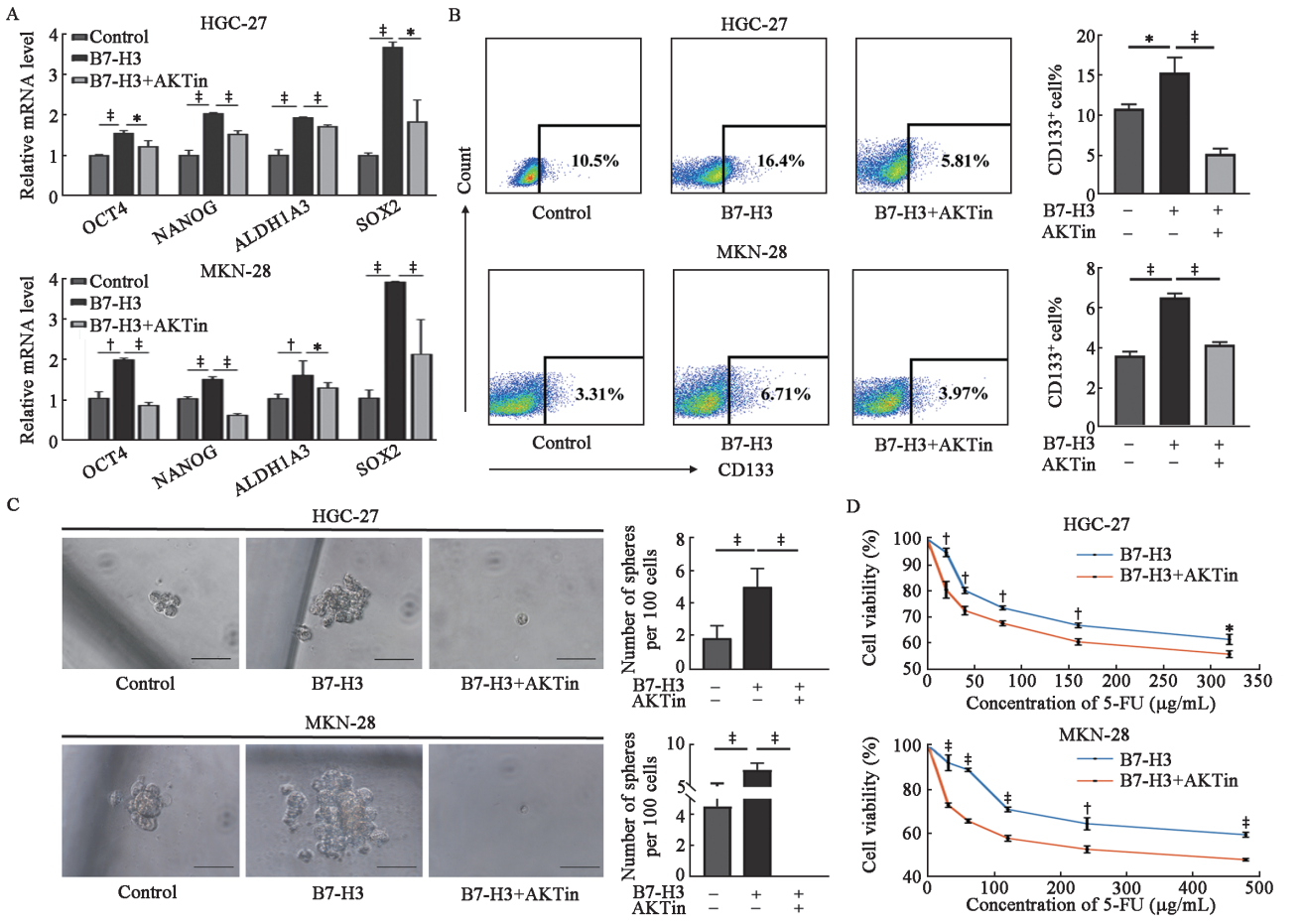

Figure 5: The AKT pathway is involved in the B7-H3-induced stemness of GC cells. (A) RT-qPCR detection of cancer stemness-related genes in B7-H3-overexpressing HGC-27 and MKN-28 cell lines after treatment with AKTin. (B) Flow cytometry analysis of CD133 expression on B7-H3-overexpressing HGC-27 and MKN-28 cell lines after treatment with AKTin. (C) Images and numbers of spheres of B7-H3-overexpressing HGC-27 and MKN-28 cell lines after treatment with AKTin. Scale bar, 50 μm. (D) B7-H3 overexpressing HGC-27 and MKN-28 cells and B7-H3 + AKTin HGC-27 and MKN-28 cells were treated with 5-FU at the indicated concentration for 24 h. Cell viability was tested by CCK8 assay. The data are presented as the mean ± SDs. $^{*}P$ <0.05, $^{\dagger}P$ <0.01, $^{\ddagger}P$ <0.001. AKT: Protein kinase B; AKTin: AKT inhibitor; ALDH1A3: Aldehyde dehydrogenase 1 A3; CD: Cluster of differentiation; 5-FU: 5-Fluorouracil; GC: Gastric cancer; mRNA: Messenger RNA; NANOG: Nanog homeobox; OCT4: Octamer-binding transcription factor; RT-qPCR: Real time quantitative polymerase chain reaction; SDs: Standard deviations; Sox2: SRY-box transcription factor 2.

Discussion

CSCs are a small subset of cancer cells with stem-like properties and have been proposed to interpret tumor progression, recurrence, and therapeutic resistance.[36,37] The stemness of tumor cells can be regulated in multiple ways including classic pathways, epigenetic modification, and metabolism alteration. A previous study showed that CD73 could sustain cancer cell stemness by promoting the transcription and stability of SOX9 in an AKT/GSK3β-dependent manner.[38] Oncostatin M (OSM) can promote cancer cell stemness through the STAT3-SMAD3 pathway.[39] There is evidence suggesting that CSC formation relies on methylation deletion in the promoter region of *NANOG*.[40] Interestingly, a high level of lysine methyltransferase 9 (KMT9), a novel histone lysine methyltransferase, promotes the maintenance and function of CSCs.[41] Accumulating evidence has suggested that metabolic alterations also play an important role in the regulation of cancer stemness.[42,43] For example, overexpression of SET domain containing 5 (SETD5), a histone lysine methyltransferase, activated glycolysis in breast CSCs and in turn increased tumor growth.[44] The long noncoding ROPM-PLA2G16 signaling axis promotes the lipid metabolism of CSCs, which is eventually involved in the maintenance of CSC stemness in breast cancer.[45] Moreover, Mukha *et al*[46] reported that glutamine catabolism modulated alpha-ketoglutarate (α-KG) -dependent chromatin-modifying dioxygenase and led to the maintenance of CSCs. However, the role of metabolic alterations in the regulation of the maintenance of cancer stemness in GC remains largely unclear. Previous studies have reported that B7-H3, as an oncogene, is involved in the progression of a variety of tumors. For example, B7-H3 inhibited doxorubicin-induced cellular senescence-like growth of colorectal cancer and promoted tumor progression.[29] Shi *et al*[47] showed that B7-H3 was highly expressed in metastatic castrate-resistant prostate cancer. Another study showed that B7-H3 contributed to ovarian cancer development by suppressing anti-tumor immunity.[48] In the current study, we observed that B7-H3 knockdown suppressed the stem-like properties of GC cells. Moreover, B7-H3 was highly expressed

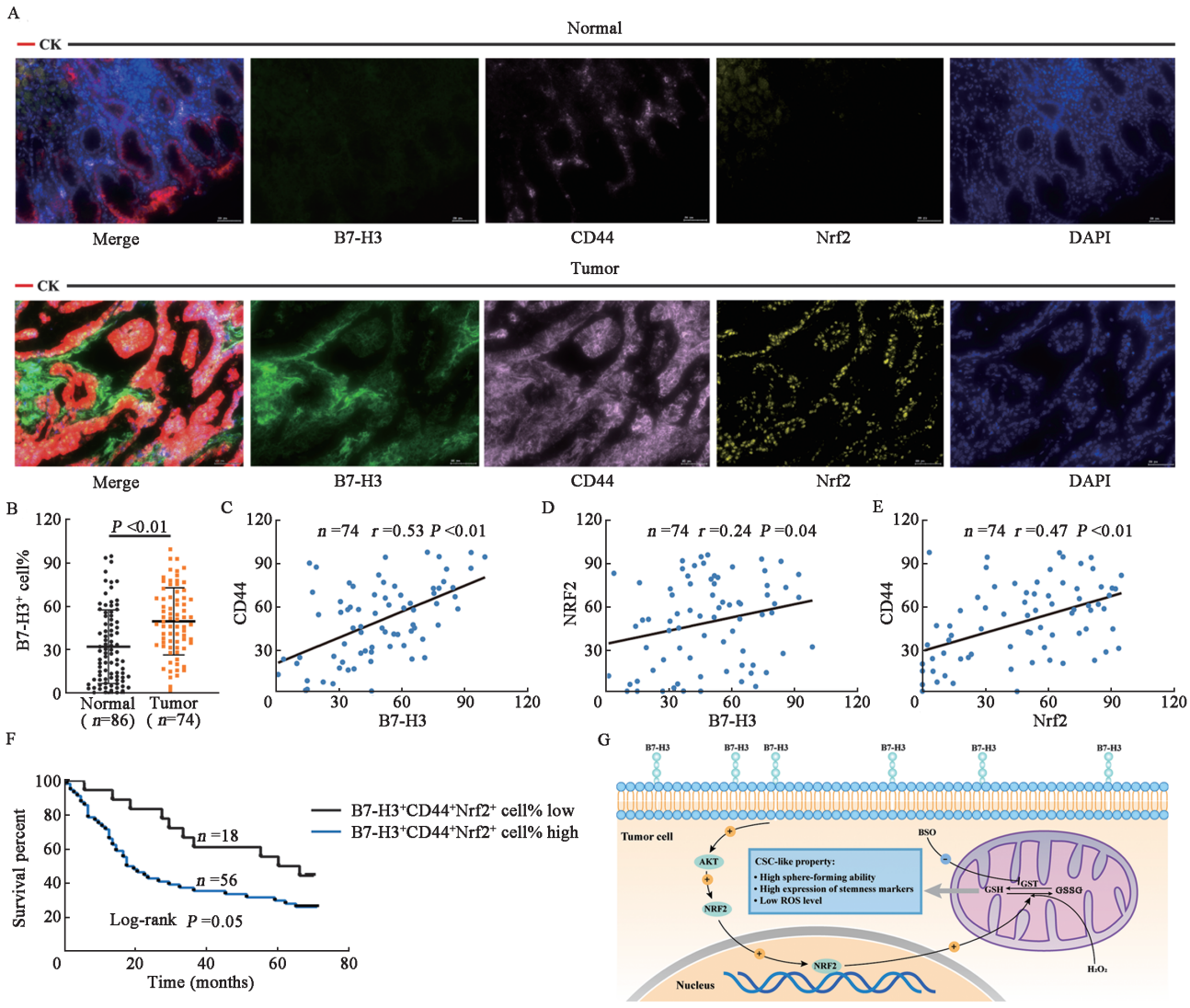

Figure 6: B7-H3 is highly expressed in GC tissue and is correlated with the expression of CD44 and Nrf2 as well as the prognosis of GC patients. (A) Expression of B7-H3 (green), CD44 (purple), and Nrf2 (yellow) in normal adjacent tissue and tumor tissue. Nuclei and tumor epithelial cells were marked by DAPI (blue) and CK (red), respectively. Scale bar, 50 μm. (B) B7-H3 expression based on B7-H3$^+$% in GC specimens and normal adjacent tissues. (C–E) Correlation analyses of B7-H3 and CD44, B7-H3 and Nrf2, and Nrf2 and CD44 in human specimens ($n = 74$). (F) Kaplan–Meier curve for overall survival in GC patients with high B7-H3$^+$CD44$^+$Nrf2$^+$ cell% or low B7-H3$^+$CD44$^+$Nrf2$^+$ cell%. The cutoff point was based on the lower quartile. (G) Schematic representation of the mechanism by which B7-H3 regulates GC stemness. AKT: Protein kinase B; BSO: Buthionine sulfoximine; CK: cytokeratin; DAPI: 4-6-Diamidino-2-phenylindole; GC: Gastric cancer; GSH: Glutathione; GSSG: Glutathione, oxydized; GST: Glutathione S transferase; ROS: Reactive oxygen species.

in the tissues of patients with GC and positively associated with CD44 expression. These results suggest that B7-H3 is an important regulator of GC cell stemness.

Multiple studies have shown that excess GSH promotes tumor progression in multiple ways, such as strengthening EMT and chemoresistance and promoting cancer cell growth.[49,50] With respect to the maintenance of cancer stemness, GSH also plays an irreplaceable role. One study on pancreatic cancer showed that GSH metabolism was essential for the chemoresistance and self-renewal of pancreatic cancer stem cells. The upregulated GSH-related genes were related to reduced disease-free survival in patients.[51] Lu *et al*[52] reported that HIF-1-dependent GSH synthesis and copper chelation could induce the stem cell phenotype of breast cancer. Furthermore, studies have shown that key enzymes in the GSH metabolic pathway also play an important role in maintaining tumor stemness. In one study, it was shown that GSTO1 inhibition could significantly decrease the invasion, migration, and mammosphere formation in breast cancer stem cells.[53] In another study, Peng *et al*[54] reported that the knockdown of GPX4 could arrest the cell cycle at G_1/G_0 phase; and inhibit cell proliferation and the stemness phenotype in Panc-1 CSCs. Moreover, dual pharmacological inhibition of thioredoxin and GSH systems could act synergistically to kill colorectal cancer stem cells.[55] In addition, nanoparticles containing GSH were capable of targeting N6-methyladenosine FTO demethylase and therefore against leukemic stem cells.[56] In this study, we found that GSH metabolism was significantly inhibited in GC cells after knocking down the expression of B7-H3. More importantly, blockade of GSH metabolism by BSO, an inhibitor of

GSH synthesis, markedly reversed the effect of B7-H3 on the stemness of GC cells.

Nrf2 is a master transcription factor that regulates the antioxidant response and maintains cellular redox homeostasis.[57] Under normal circumstances, Nrf2 binds to KEAP1, which enables continuous degradation of Nrf2 by the proteasome. Under oxidative stress conditions, KEAP1 is oxidized, and Nrf2 is translocated into the nucleus and activates different genes.[58] It is well known that NRF2 signaling plays an important role in the regulation of GSH metabolism, as evidenced by the transcriptional control of the expression of GSH metabolism-related enzymes, such as glutamate-cysteine catalytic subunit (GCLC), glutathione peroxidase (GPX), and GST.[59,60] Moreover, the increased transcriptional activity of Nrf2 could promote GSH production, and therefore sustain the redox homeostasis and survival of cancer cells.[61,62] In the current study, knockdown of B7-H3 significantly reduced the Nrf2 expression in GC cells. Moreover, the Nrf2 activator SFN significantly increased the GSH level and GST enzyme activity of GC cells, which decreased after B7-H3 knockdown. Importantly, we observed that Nrf2 expression was positively associated with the expression of B7-H3 and CD44 in GC clinical samples. These data suggest that B7-H3 promotes GSH metabolism in an Nrf2-dependent manner.

The AKT pathway exerts critical effects on several biological functions including cell proliferation, stemness, and GSH metabolism.[63,64] The PI3K/AKT axis promoted the biosynthesis of GSH by stabilizing and activating Nrf2 to increase GSH biosynthetic genes in mammary epithelial cells.[65] Li *et al*[66] showed that glutamic-oxaloacetic transaminase 2 (GOT2) knockdown elevated glutaminolysis, nucleotide synthesis, and GSH synthesis, resulting in the reprograming of glutamine metabolism to support the cellular antioxidant system, and the regulation of hepatocellular carcinoma progression through the phosphoinositide 3-kinase (PI3K)/AKT/mammalian target of rapamycin (mTOR) pathway. Additionally, the activation of PI3K/Akt/mTOR signaling was involved in the EMT and CSC marker expression in chemoresistant epithelial ovarian cancer cells.[67] Moreover, silencing transmembrane and coiled-coil domain family 3 (TMCC3) reduced AKT activation and inhibited the self-renewal and metastasis of breast cancer stem cells.[68] Herein, our data showed that B7-H3 overexpression elevated p-AKT and Nrf2 protein expression. Furthermore, perifosine treatment reversed the effect of B7-H3 on GSH metabolism and the stemness of GC cells. Notably, there are few reports on how B7-H3 regulates Nrf2 expression, and the underlying mechanism needs to be further investigated.

Although our study has elucidated the mechanism by which B7-H3 regulates the stemness of GC, it still has some limitations. First, the current study comprised only 74 GC patients. Given that the sample size was relatively small, the significance of our study is limited. Second, though we examined some characteristics related to cancer stemness, we did not directly isolate GC stem cells. Therefore, further investigations are needed in a larger population to elucidate the expression pattern and clinical significance, and further isolation of GC stem cells is needed for stemness-related examination.

In summary, our study explored the regulatory role of B7-H3 in the stemness of GC cells [Figure 6G]. We revealed that B7-H3 controlled the stemness of GC cells through GSH metabolism, which was promoted by the AKT/Nrf2 pathway [Figure 6G]. Therefore, our findings uncover a novel mechanism by which B7-H3 regulates the stemness of GC, suggesting that B7-H3 may act not only as a new biomarker for the diagnosis and prognosis of GC patients but also as a target for GC treatment.

Funding

This study was supported by Suzhou Special Project on Clinical Key Diseases Treatment Technology of Suzhou Commission of Health (No. LCZX201803); People's Livelihood and Science and Technology project of Department of Science and Technology of Suzhou (No. SS2019059); Jiangsu Provincial Medical Key Discipline (No. ZDXK202246); Key Project of Jiangsu Provincial Health Commission (No. zd2021050); the Natural Science Foundation of the Jiangsu Higher Education Institutions of China (No. 20KJA310005); Key Project of Medical Research of Jiangsu Commission of Health (No. ZDA2020008); National Natural Science Foundation of China (No. 81802843); and Social Development Project of Department of Science and Technology of Jiangsu Province (No. BE2019667).

Conflicts of interest

None.

References

1. Xia C, Dong X, Li H, Cao M, Sun D, He S, *et al*. Cancer statistics in China and United States, 2022: Profiles, trends, and determinants. Chin Med J 2022;135:584–590. doi: 10.1097/CM9.0000000000002108.
2. Ajani JA, D'Amico TA, Bentrem DJ, Chao J, Cooke D, Corvera C, *et al*. Gastric cancer, version 2.2022, NCCN clinical practice guidelines in oncology. J Natl Compr Canc Netw 2022;20:167–192. doi: 10.6004/jnccn.2022.0008.
3. Joshi SS, Badgwell BD. Current treatment and recent progress in gastric cancer. CA Cancer J Clin 2021;71:264–279. doi: 10.3322/caac.21657.
4. Najafi M, Mortezaee K, Majidpoor J. Cancer stem cell (CSC) resistance drivers. Life Sci 2019;234:116781. doi: 10.1016/j.lfs.2019.116781.
5. Yu Z, Pestell TG, Lisanti MP, Pestell RG. Cancer stem cells. Int J Biochem Cell Biol 2012;44:2144–2151. doi: 10.1016/j.biocel.2012.08.022.
6. Vasquez EG, Nasreddin N, Valbuena GN, Mulholland EJ, Belnoue-Davis HL, Eggington HR, *et al*. Dynamic and adaptive cancer stem cell population admixture in colorectal neoplasia. Cell Stem Cell 2022;29:1213.e–1228.e. doi: 10.1016/j.stem.2022.07.008.
7. Chen X, Yang M, Yin J, Li P, Zeng S, Zheng G, *et al*. Tumor-associated macrophages promote epithelial-mesenchymal transition and the cancer stem cell properties in triple-negative breast cancer through CCL2/AKT/β-catenin signaling. Cell Commun Signal 2022;20:92. doi: 10.1186/s12964-022-00888-2.
8. Zhao R, He B, Bie Q, Cao J, Lu H, Zhang Z, *et al*. AQP5 complements LGR5 to determine the fates of gastric cancer stem cells through regulating ULK1 ubiquitination. J Exp Clin Cancer Res 2022;41:322. doi: 10.1186/s13046-022-02532-w.

9. Xiang R, Song W, Ren J, Wu J, Fu J, Fu T. Identification of stem cell-related subtypes and risk scoring for gastric cancer based on stem genomic profiling. Stem Cell Res Ther 2021;12:563. doi: 10.1186/s13287-021-02633-x.
10. Liu S, Liang J, Liu Z, Zhang C, Wang Y, Watson AH, *et al*. The role of CD276 in cancers. Front Oncol 2021;11:654684. doi: 10.3389/fonc.2021.654684.
11. Yonesaka K, Haratani K, Takamura S, Sakai H, Kato R, Takegawa N, *et al*. B7-H3 negatively modulates CTL-mediated cancer immunity. Clin Cancer Res 2018;24:2653–2664. doi: 10.1158/1078-0432.CCR-17-2852.
12. Ulase D, Behrens HM, Krüger S, Zeissig S, Röcken C. Gastric carcinomas with stromal B7-H3 expression have lower intratumoural CD8+ T cell density. Int J Mol Sci 2021;22:2129. doi: 10.3390/ijms22042129.
13. Castellanos JR, Purvis IJ, Labak CM, Guda MR, Tsung AJ, Velpula KK, *et al*. B7-H3 role in the immune landscape of cancer. Am J Clin Exp Immunol 2017;6:66–75.
14. Zhou L, Zhao Y. B7-H3 induces ovarian cancer drugs resistance through an PI3K/AKT/BCL-2 signaling pathway. Cancer Manag Res 2019;11:10205–10214. doi: 10.2147/CMAR.S222224.
15. Wang R, Ma Y, Zhan S, Zhang G, Cao L, Zhang X, *et al*. B7-H3 promotes colorectal cancer angiogenesis through activating the NF-κB pathway to induce VEGFA expression. Cell Death Dis 2020;11:55. doi: 10.1038/s41419-020-2252-3.
16. Wu J, Wang F, Liu X, Zhang T, Liu F, Ge X, *et al*. Correlation of IDH1 and B7H3 expression with prognosis of CRC patients. Eur J Surg Oncol 2018;44:1254–1260. doi: 10.1016/j.ejso.2018.05.005.
17. Nehama D, Di Ianni N, Musio S, Du H, Patané M, Polloc B, *et al*. B7-H3-redirected chimeric antigen receptor T cells target glioblastoma and neurospheres. EBioMedicine 2019;47:33–43. doi: 10.1016/j.ebiom.2019.08.030.
18. Zhang Y, He L, Sadagopan A, Ma T, Dotti G, Wang Y, *et al*. Targeting radiation-resistant prostate cancer stem cells by B7-H3 CAR T cells. Mol Cancer Ther 2021;20:577–588. doi: 10.1158/1535-7163.Mct-20-0446.
19. Wang C, Li Y, Jia L, Kim JK, Li J, Deng P, *et al*. CD276 expression enables squamous cell carcinoma stem cells to evade immune surveillance. Cell Stem Cell 2021;28:1597–1613.e7. doi: 10.1016/j.stem.2021.04.011.
20. Liu Z, Zhang W, Phillips JB, Arora R, McClellan S, Li J, *et al*. Immunoregulatory protein B7-H3 regulates cancer stem cell enrichment and drug resistance through MVP-mediated MEK activation. Oncogene 2019;38:88–102. doi: 10.1038/s41388-018-0407-9.
21. Shi H, Yang Y. Identification of inhibitory immune checkpoints and relevant regulatory pathways in breast cancer stem cells. Cancer Med 2021;10:3794–3807. doi: 10.1002/cam4.3902.
22. Wen B, Mei Z, Zeng C, Liu S. metaX: a flexible and comprehensive software for processing metabolomics data. BMC Bioinformatics 2017;18:183. doi: 10.1186/s12859-017-1579-y.
23. Shi T, Ma Y, Cao L, Zhan S, Xu Y, Fu F, *et al*. B7-H3 promotes aerobic glycolysis and chemoresistance in colorectal cancer cells by regulating HK2. Cell Death Dis 2019;10:308. doi: 10.1038/s41419-019-1549-6.
24. Nelson JK, ThinMZ, EvanT, HowellS, WuM, AlmeidaB, et al. USP25 promotes pathological HIF-1-driven metabolic reprogramming and is a potential therapeutic target in pancreatic cancer. Nat Commun 2022;13:2070. doi: 10.1038/s41467-022-29684-9.
25. Saha SK, Parachoniak CA, Bardeesy N. IDH mutations in liver cell plasticity and biliary cancer. Cell Cycle 2014;13:3176–3182. doi: 10.4161/15384101.2014.965054.
26. Hu S, Sechi M, Singh PK, Dai L, McCann S, Sun D, *et al*. A novel redox modulator induces a GPX4-mediated cell death that is dependent on iron and reactive oxygen species. J Med Chem 2020;63:9838–9855. doi: 10.1021/acs.jmedchem.0c01016.
27. Jogo T, Oki E, Nakanishi R, Ando K, Nakashima Y, Kimura Y, *et al*. Expression of CD44 variant 9 induces chemoresistance of gastric cancer by controlling intracellular reactive oxygen spices accumulation. Gastric Cancer 2021;24:1089–1099. doi: 10.1007/s10120-021-01194-5.
28. Sayin VI, LeBoeuf SE, Singh SX, Davidson SM, Biancur D, Guzelhan BS, *et al*. Activation of the NRF2 antioxidant program generates an imbalance in central carbon metabolism in cancer. Elife 2017;6:e28083. doi: 10.7554/eLife.28083.
29. Sporn MB, Liby KT. NRF2 and cancer: The good, the bad and the importance of context. Nat Rev Cancer 2012;12:564–571. doi: 10.1038/nrc3278.
30. Kamble D, Mahajan M, Dhat R, Sitasawad S. Keap1-Nrf2 pathway regulates ALDH and contributes to radioresistance in breast cancer stem cells. Cells 2021;10:83. doi: 10.3390/cells10010083.
31. Park J, Kim SK, Hallis SP, Choi BH, Kwak MK. Role of CD133/NRF2 axis in the development of colon cancer stem cell-like properties. Front Oncol 2022;11:808300. doi: 10.3389/fonc.2021.808300.
32. Gambardella V, Gimeno-Valiente F, Tarazona N, Martinez-Ciarpaglini C, Roda D, Fleitas T, *et al*. NRF2 through RPS6 activation is related to anti-HER2 drug resistance in *HER2*-amplified gastric cancer. Clin Cancer Res 2019;25:1639–1649. doi: 10.1158/1078-0432.Ccr-18-2421.
33. Liu JZ, Hu YL, Feng Y, Jiang Y, Guo YB, Liu YF, *et al*. BDH2 triggers ROS-induced cell death and autophagy by promoting Nrf2 ubiquitination in gastric cancer. J Exp Clin Cancer Res 2020;39:123. doi: 10.1186/s13046-020-01620-z.
34. Wang R, Sun L, Xia S, Wu H, Ma Y, Zhan S, *et al*. B7-H3 suppresses doxorubicin-induced senescence-like growth arrest in colorectal cancer through the AKT/TM4SF1/SIRT1 pathway. Cell Death Dis 2021;12:453. doi: 10.1038/s41419-021-03736-2.
35. Sun M, Xie J, Zhang D, Chen C, Lin S, Chen Y, *et al*. B7-H3 inhibits apoptosis of gastric cancer cell by interacting with fibronectin. J Cancer 2021;12:7518–7526. doi: 10.7150/jca.59263.
36. Atashzar MR, Baharlou R, Karami J, Abdollahi H, Rezaei R, Pourramezan F, *et al*. Cancer stem cells: A review from origin to therapeutic implications. J Cell Physiol 2020;235:790–803. doi: 10.1002/jcp.29044.
37. Yuan S, Stewart KS, Yang Y, Abdusselamoglu MD, Parigi SM, Feinberg TY, *et al*. Ras drives malignancy through stem cell crosstalk with the microenvironment. Nature 2022;612:555–563. doi: 10.1038/s41586-022-05475-6.
38. Ma XL, Hu B, Tang WG, Xie SH, Ren N, Guo L, *et al*. CD73 sustained cancer-stem-cell traits by promoting SOX9 expression and stability in hepatocellular carcinoma. J Hematol Oncol 2020;13:11. doi: 10.1186/s13045-020-0845-z.
39. Junk DJ, Bryson BL, Smigiel JM, Parameswaran N, Bartel CA, Jackson MW. Oncostatin M promotes cancer cell plasticity through cooperative STAT3-SMAD3 signaling. Oncogene 2017;36:4001–4013. doi: 10.1038/onc.2017.33.
40. Liu S, Cheng K, Zhang H, Kong R, Wang S, Mao C, *et al*. Methylation status of the *Nanog* promoter determines the switch between cancer cells and cancer stem cells. Adv Sci (Weinh) 2020;7:1903035. doi: 10.1002/advs.201903035.
41. Berlin C, Cottard F, Willmann D, Urban S, Tirier SM, Marx L, *et al*. KMT9 controls stemness and growth of colorectal cancer. Cancer Res 2022;82:210–220. doi: 10.1158/0008-5472.CAN-21-1261.
42. Zhang Y, Liu Y, Lang F, Yang C. IDH mutation and cancer stem cell. Essays Biochem 2022;66:413–422. doi: 10.1042/EBC20220008.
43. Chong KH, Chang YJ, Hsu WH, Tu YT, Chen YR, Lee MC, *et al*. Breast cancer with increased drug resistance, invasion ability, and cancer stem cell properties through metabolism reprogramming. Int J Mol Sci 2022;23:12875. doi: 10.3390/ijms232112875.
44. Yang Z, Zhang C, Liu X, Che N, Feng Y, Xuan Y. SETD5 regulates glycolysis in breast cancer stem-like cells and fuels tumor growth. Am J Pathol 2022;192:712–721. doi: 10.1016/j.ajpath.2021.12.006.
45. Liu S, Sun Y, Hou Y, Yang L, Wan X, Qin Y, *et al*. A novel lncRNA ROPM-mediated lipid metabolism governs breast cancer stem cell properties. J Hematol Oncol 2021;14:178. doi: 10.1186/s13045-021-01194-z.
46. Mukha A, Kahya U, Linge A, Chen O, Löck S, Lukiyanchuk V, *et al*. GLS-driven glutamine catabolism contributes to prostate cancer radiosensitivity by regulating the redox state, stemness and ATG5-mediated autophagy. Theranostics 2021;11:7844–7868.doi: 10.7150/thno.58655.
47. Shi X, Day A, Bergom HE, Tape S, Baca SC, Sychev ZE, *et al*. Integrative molecular analyses define correlates of high B7-H3 expression in metastatic castrate-resistant prostate cancer. NPJ Precis Oncol 2022;6:80. doi: 10.1038/s41698-022-00323-2.
48. Miyamoto T, Murakami R, Hamanishi J, Tanigaki K, Hosoe Y, Mise N, *et al*. B7-H3 suppresses antitumor immunity via the CCL2-CCR2-M2 macrophage axis and contributes to ovarian cancer progression. Cancer Immunol Res 2022;10:56–69. doi: 10.1158/2326-6066.CIR-21-0407.
49. Luo Y, Xiang W, Liu Z, Yao L, Tang L, Tan W, *et al*. Functional role of the SLC7A11-AS1/xCT axis in the development of gastric

cancer cisplatin-resistance by a GSH-dependent mechanism. Free Radic Biol Med 2022;184:53–65. doi: 10.1016/j.freeradbiomed.2022.03.026.
50. Ogata FT, Simões Sato AY, Coppo L, Arai RJ, Stern AI, Pequeno Monteiro H. Thiol-based antioxidants and the epithelial/mesenchymal transition in cancer. Antioxid Redox Signal 2022;36:1037–1050. doi: 10.1089/ars.2021.0199.
51. Jagust P, Alcalá S, Sainz B Jr., Heeschen C, Sancho P. Glutathione metabolism is essential for self-renewal and chemoresistance of pancreatic cancer stem cells. World J Stem Cells 2020;12:1410–1428. doi: 10.4252/wjsc.v12.i11.1410.
52. Lu H, Samanta D, Xiang L, Zhang H, Hu H, Chen I, *et al*. Chemotherapy triggers HIF-1-dependent glutathione synthesis and copper chelation that induces the breast cancer stem cell phenotype. Proc Natl Acad Sci U S A 2015;112:E4600–E4609. doi: 10.1073/pnas.1513433112.
53. Manupati K, Debnath S, Goswami K, Bhoj PS, Chandak HS, Bahekar SP, *et al*. Glutathione S-transferase omega 1 inhibition activates JNK-mediated apoptotic response in breast cancer stem cells. FEBS J 2019;286:2167–2192. doi: 10.1111/febs.14813.
54. Peng G, Tang Z, Xiang Y, Chen W. Glutathione peroxidase 4 maintains a stemness phenotype, oxidative homeostasis and regulates biological processes in Panc1 cancer stemlike cells. Oncol Rep 2019;41:1264–1274. doi: 10.3892/or.2018.6905.
55. Tanaka G, Inoue K, Shimizu T, Akimoto K, Kubota K. Dual pharmacological inhibition of glutathione and thioredoxin systems synergizes to kill colorectal carcinoma stem cells. Cancer Med 2016;5:2544–2557. doi: 10.1002/cam4.844.
56. Cao K, Du Y, Bao X, Han M, Su R, Pang J, *et al*. Glutathione-bioimprinted nanoparticles targeting of N6-methyladenosine FTO demethylase as a strategy against leukemic stem cells. Small 2022;18:e2106558. doi: 10.1002/smll.202106558.
57. Panieri E, Pinho SA, Afonso GJM, Oliveira PJ, Cunha-Oliveira T, Saso L. NRF2 and mitochondrial function in cancer and cancer stem cells. Cells 2022;11:2401. doi: 10.3390/cells11152401.
58. Jaramillo MC, Zhang DD. The emerging role of the Nrf2-Keap1 signaling pathway in cancer. Genes Dev 2013;27:2179–2191. doi: 10.1101/gad.225680.113.
59. Zhang HX, Chen Y, Xu R, He QY. Nrf2 mediates the resistance of human A549 and HepG2 cancer cells to boningmycin, a new antitumor antibiotic, in vitro through regulation of glutathione levels. Acta Pharmacol Sin 2018;39:1661–1669. doi: 10.1038/aps.2018.21.
60. Krajka-Kuz niak V, Paluszczak J, Baer-Dubowska W. The Nrf2-ARE signaling pathway: An update on its regulation and possible role in cancer prevention and treatment. Pharmacol Rep 2017;69:393–402. doi: 10.1016/j.pharep.2016.12.011.
61. Zhang W, Li X, Xu J, Wang Y, Xing Z, Hu S, *et al*. The RSL3 induction of *KLK* lung adenocarcinoma cell ferroptosis by inhibition of USP11 activity and the NRF2-GSH axis. Cancers (Basel) 2022;14:5233. doi: 10.3390/cancers14215233.
62. Sun R, Liu M, Xu K, Pu Y, Huang J, Liu J, *et al*. Ferroptosis is involved in the benzene-induced hematotoxicity in mice via iron metabolism, oxidative stress and NRF2 signaling pathway. Chem Biol Interact 2022;362:110004. doi: 10.1016/j.cbi.2022.110004.
63. Dong S, Liang S, Cheng Z, Zhang X, Luo L, Li L, *et al*. ROS/PI3K/Akt and Wnt/β-catenin signalings activate HIF-1α-induced metabolic reprogramming to impart 5-fluorouracil resistance in colorectal cancer. J Exp Clin Cancer Res 2022;41:15. doi: 10.1186/s13046-021-02229-6.
64. Xu JC, Chen TY, Liao LT, Chen T, Li QL, Xu JX, *et al*. NETO2 promotes esophageal cancer progression by inducing proliferation and metastasis via PI3K/AKT and ERK pathway. Int J Biol Sci 2021;17:259–270. doi: 10.7150/ijbs.53795.
65. Lien EC, Lyssiotis CA, Juvekar A, Hu H, Asara JM, Cantley LC, *et al*. Glutathione biosynthesis is a metabolic vulnerability in PI(3)K/Akt-driven breast cancer. Nat Cell Biol 2016;18:572–578. doi: 10.1038/ncb3341.
66. Li Y, Li B, Xu Y, Qian L, Xu T, Meng G, *et al*. GOT2 silencing promotes reprogramming of glutamine metabolism and sensitizes hepatocellular carcinoma to glutaminase inhibitors. Cancer Res 2022;82:3223–3235. doi: 10.1158/0008-5472.CAN-22-0042.
67. Deng J, Bai X, Feng X, Ni J, Beretov J, Graham P, *et al*. Inhibition of PI3K/Akt/mTOR signaling pathway alleviates ovarian cancer chemoresistance through reversing epithelial-mesenchymal transition and decreasing cancer stem cell marker expression. BMC Cancer 2019;19:618. doi: 10.1186/s12885-019-5824-9.
68. Wang YH, Chan YT, Hung TH, Hung JT, Kuo MW, Wang SH, *et al*. Transmembrane and coiled-coil domain family 3 (TMCC3) regulates breast cancer stem cell and AKT activation. Oncogene 2021;40:2858–2871. doi: 10.1038/s41388-021-01729-1.

How to cite this article: Xia L, Chen YQ, Li JT, Wang JY, Shen KE, Zhao AJ, Jin HY, Zhang GB, Xi QH, Xia SH, Shi TG, Li R. B7-H3 confers stemness characteristics to gastric cancer cells by promoting glutathione metabolism through AKT/pAKT/Nrf2 pathway. Chin Med J 2023;136:1977–1989. doi: 10.1097/CM9.0000000000002772